ELSEVIER

NeuroImage

www.elsevier.com/locate/ynimg
NeuroImage 42 (2008) 112–121

A study of the brain's resting state based on alpha band power, heart rate and fMRI

J.C. de Munck,[a,*] S.I. Gonçalves,[a] Th.J.C. Faes,[a] J.P.A. Kuijer,[a] P.J.W. Pouwels,[a] R.M. Heethaar,[a] and F.H. Lopes da Silva[b]

[a]*Department PMT, VU Medical Center, De Boelelaan 1117, 1081 HV Amsterdam, The Netherlands*
[b]*Swammerdam Institute for Life Sciences, University of Amsterdam, Amsterdam, The Netherlands*

Received 25 October 2007; revised 14 February 2008; accepted 17 April 2008
Available online 2 May 2008

Considering that there are several theoretical reasons why fMRI data is correlated to variations in heart rate, these correlations are explored using experimental resting state data. In particular, the possibility is discussed that the "default network", being a brain area that deactivates during non-specific general tasks, is a hemodynamic effect caused by heart rate variations.

Of fifteen healthy controls ECG, EEG and fMRI were co-registered. Slice time dependent heart rate regressors were derived from the ECG data and correlated to fMRI using a linear correlation analysis where the impulse response is estimated from the data.

It was found that in most subjects substantial correlations between heart rate variations and fMRI exist, both within the brain and at the ventricles. The brain areas with high correlation to heart rate are different from the "default network" and the response functions deviate from the canonical hemodynamic response function. Furthermore, a general negative correlation was found between heart beat intervals (reverse of heart rate) and alpha power. We interpret this finding by assuming that subject's state varies between drowsiness and wakefulness. Finally, given this large correlation, we re-examined the contribution of heart rate variations to earlier reported fMRI/alpha band correlations, by adding heart rate regressors as confounders. It was found that inclusion of these confounders most often had a negligible effect.

From its strong correlation to alpha power, we conclude that the heart rate variations contain important physiological information about subject's resting state. However, it does not provide a full explanation of the behaviour of the "default network". Its application as confounder in fMRI experiments is a relatively small computational effort, but may have a substantial impact in paradigms where heart rate is controlled by the stimulus.

Introduction

MR technology provides several ways to localise brain activity related to an external stimulus or task (Kwong, 1995). The physical principle underlying fMRI is based on a difference in T2*-relaxation times between an active and a control state (Ogawa et al., 1992). In the active state, the local cerebral blood flow (CBF) increases much more than the cerebral metabolic rate of oxygen, and as a result the local extraction oxygen fraction decreases (Fox and Raichle, 1986), deoxyhemoglobin concentration in the venules decreases, the local field homogeneity increases and, as a result, also the magnetic resonance signal (Buxton et al., 2004) increases. This mechanism constitutes the blood oxygenation level dependent (BOLD) signal.

Although these principles are broadly accepted, some controversy has recently arisen on the precise meaning of the resting state, commonly used as control state to which an activated state is compared (Buckner and Vincent, 2007 versus Morcom and Fletcher, 2007). By comparing flow contrasts derived from tracer kinetic modelling of PET data, Shulman et al. (1997) and later Mazoyer et al. (2001) have found a spatially quite consistent *decrease* in cerebral blood flow in several types of activation studies compared with resting state. This is the case for brain regions comprising the posterior cingulate (PCC) and ventral anterior cingulate cortex (vACC), and the bilateral inferior parietal cortices. Raichle et al. (2001) introduced the term "default network", based on PET measurements, considering that these brain regions would form a network that is active in rest – the default mode – and shows decreased activity during the performance of attention demanding cognitive tasks. Greicius et al. (2003), employing correlation analysis to fMRI data, found that the brain areas comprising the "default mode network" were strongly coupled. This finding was confirmed using spatially independent component analysis (Damoiseaux et al., 2006), and Vincent et al. (2007) reported similar correlation structures in anaesthetized monkeys. Raichle et al. (2001) observed that for a subject at rest the oxygen extraction fraction is very homogeneously distributed over the brain. In particular, no significant differences appeared to exist between the formerly

* Corresponding author.
E-mail address: jc.demunck@vumc.nl (J.C. de Munck).
Available online on ScienceDirect (www.sciencedirect.com).

1053-8119/$ - see front matter © 2008 Elsevier Inc. All rights reserved.
doi:10.1016/j.neuroimage.2008.04.244

mentioned deactivation regions and the rest of the brain. Thus Raichle et al. (2001) concluded that deactivation of the default network should be interpreted as a reallocation of resources from default functions to goal directed functional states (Gusnard and Raichle, 2001; Raichle and Snyder, 2007).

However, contrary to PET dynamic modelling, which yields a quantitave measure of local cerebral blood flow (Herscovitch et al., 1973), fMRI T2* imaging only yields an indirect measure of brain activity. Temporal fluctuations of fMRI signals in a resting state condition result from a combination of neural activity filtered by a hemodynamic response function (Logothetis et al., 2001), and physiological variables ("physiological noise") like respiration, cardiac activity and motion (e.g. Glover et al., 2000; Lund et al., 2006), as well as non-physiological noise. For these reasons, the nature of the resting state fMRI analysis remains ambiguous (Logothetis, 2007), despite the fact that it corresponds closely to PET observations.

Recent technological developments (Lemieux et al., 1997, 1999) have made it possible to co-register fMRI and EEG. Such studies have improved our understanding of the fMRI resting state signal. For instance, it has been shown that the fMRI resting state signal is highly correlated to spontaneous fluctuations of the alpha rhythm (Goldman et al., 2002; Laufs et al., 2003a; Moosmann et al., 2003; Gonçalves et al., 2006; De Munck et al., 2007a), and other brain rhythms (Laufs et al., 2003b; Mantini et al., 2007). Clinically, co-registered EEG and fMRI has been used to localise the generators of inter-ictal spikes (e.g. Salek-Haddadi et al., 2003; Liston et al., 2003a; Zijlmans et al., 2007). Interestingly, Laufs et al. (2006) have found in a case study that during an absence seizure, the default network deactivates, suggesting that the decrease of activity in this network is related to the loss of consciousness.

Since EEG recorded inside an MR scanner is highly disturbed by cardiac motion (Lemieux et al., 1999), in EEG/fMRI studies the ECG or pulse is usually also recorded and used to correct the EEG. However, the beating heart also has an impact on fMRI due to moving vessels and cerebrospinal fluid, and therefore it has been also used to improve the quality of the fMRI (Liston et al., 2003b).

What has been overlooked in resting state studies based on (EEG)fMRI is that the heart rate is a physiological variable that interacts with the brain's hemodynamical state, and it is not only a source of artefacts. For example, when a subject falls asleep, characteristic EEG changes occur as well as changes in heart rate; similarly, during mental action changes in heart rate and in EEG parameters concur (Foster and Harrison, 2004). It is to be expected that even in a paradigm where a subject is instructed to lay at rest with eyes closed trying not to fall asleep, spontaneous heartbeat variations exist. We hypothesize that these heartbeat variations are correlated to the fMRI BOLD signal, for the following reasons:

- Heart rate is regulated by processes at the level of the central nervous system.
- Heart rate may affect blood volume and blood flow through hemodynamic mechanisms.
- EPI scans are sensitive to flow effects, even when a large repetition time TR is used.
- Both heart rate and alpha power contain information about a subject's resting state. It has been demonstrated that during sleep heart rate and alpha power are correlated (Ehrhart et al., 2000; Kubota et al., 2001). If such correlation also exists in a resting state experiment, this may provide an indirect way of heart rate-BOLD correlation, since the alpha band-BOLD correlation has already been demonstrated.

The correlation between heart rate and BOLD have been explored before in sleeping subjects by Shmueli et al. (2007) and in De Munck et al. (2007b) some preliminary results are presented. In the present paper EEG alpha power variations are included in the correlation analysis. Our main goal is to obtain a better understanding of the impact of heart rate variations on fMRI resting state signals. We explore the possibility that the default network may be affected by heart rate variations, given its deactivation unspecifically with several tasks. Since heart rate effects may interfere with regressors of interest in an fMRI regression analysis, a secondary goal of the present paper is to study to what extent this effect can be eliminated by incorporating heart rate covariates as nuisance regressors. We therefore re-examine the correlation between alpha band and BOLD as in De Munck et al. (2007a), but this time with heart rate regressors as confounders.

Materials and methods

Data and subjects

Subjects, data acquisition and data pre-processing were identical to those described in De Munck et al. (2007a). Briefly, co-registered EEG-fMRI data were acquired from 16 healthy subjects (7 males, mean age 27, ±9 years) while they lay in the scanner with eyes closed, resting without falling asleep, in a room that was kept in the dark. Subjects gave informed written consent prior to participation in this study, which was approved by the local ethical committee. EEG data were acquired with an MR compatible EEG amplifier (SD MRI 64, MicroMed, Treviso, Italy) and a cap providing 64 Ag/AgCl electrodes positioned according to an extended 10/20 system. EEG data were re-referenced to average reference, gradient and pulse artefacts were removed using the algorithm of Gonçalves et al. (2007) and a spectrogram was made by computing an FFT (Frigo and Johnson, 2005) every 3s, corresponding to the repetition time of the EPI sequence. For all subjects also ECG or Oxygen saturation were recorded, in most subjects we recorded both. Heart beats were detected semi-automatically and careful visual inspection was performed to correct all detections.

Functional images were acquired on a 1.5T MR scanner (Magnetom Sonata, Siemens, Erlangen, Germany) using a circularly polarized head coil. For the fMRI a T2* weighted EPI sequence was used (TR=3000 s, echo time TE=60 ms, 64×64 matrix, FOV=211×211 mm, slice thickness=3 mm (10% gap), voxel size=3.3×3.3×3 mm^3) with 24 transversal slices covering the complete occipital, parietal and frontal lobes. Slices were recorded from bottom to top, with a constant time-interval of 125 ms. In the protocol, 600 volumes were acquired, resulting in 1800s of EPI recording.

Of each subject also a T1-weighted anatomical scan (MPRAGE, TR=2700 s, TE=5 ms, inversion time TI=950 ms) was made, consisting of 160 coronal slices of 1.5 mm thickness. After motion correction, fMRI data were spatially smoothed with Gaussian kernel with standard deviation of 5 mm. Motion parameters were saved and used as confounders in the correlation analysis.

After 6 months, a second scan was obtained from subject 5, but this time with 1200s fMRI resting state. Fig. 1.

Regressors

We applied the general linear model to correlate heart rate and alpha power to fMRI BOLD. The alpha band regressors were derived by cutting a 2 Hz wide alpha band from the spectrogram, centred at

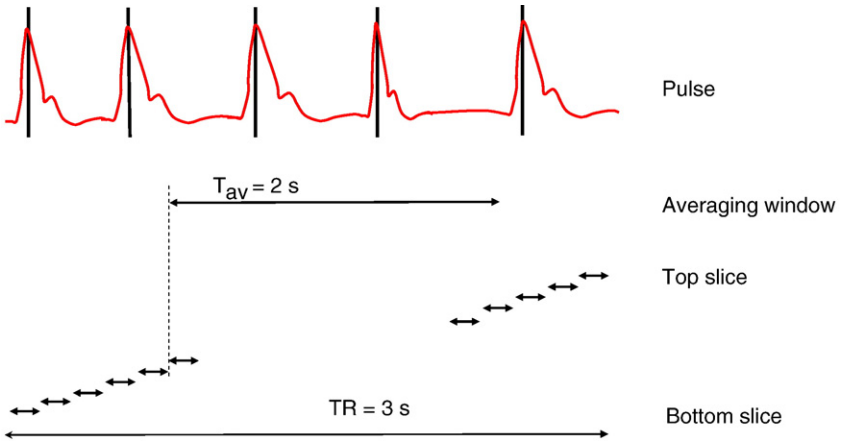

Fig. 1. The construction of the heart beat regressors is shown. The red curve is a schematic representation of the pulse signal and demonstrates the irregularity of the heart beat interval on a realistic time scale. With Glover's RETROICOR method regressors are derived from the heart beat by first determining the instantaneous phase of the heart beat at the moment a slice is recorded and then taking sine and cosine functions of this phase. Contrary to Glover's method, our heart beat interval regressors are derived from the time intervals between subsequent heart beats. For each recorded slice and each volume, a representative heart beat time is obtained by averaging all heart beat intervals (HBI) that have at least one point in common with the averaging interval T_{av} that starts at slice onset. In this example, there are three heart beat intervals overlapping with the averaging interval shown. This way of constructing regressors results in different regressors for each slice, which are intrinsically slice time corrected. Note that HBI is the inverse of heart rate. (For interpretation of the references to colour in this figure legend, the reader is referred to the web version of this article.)

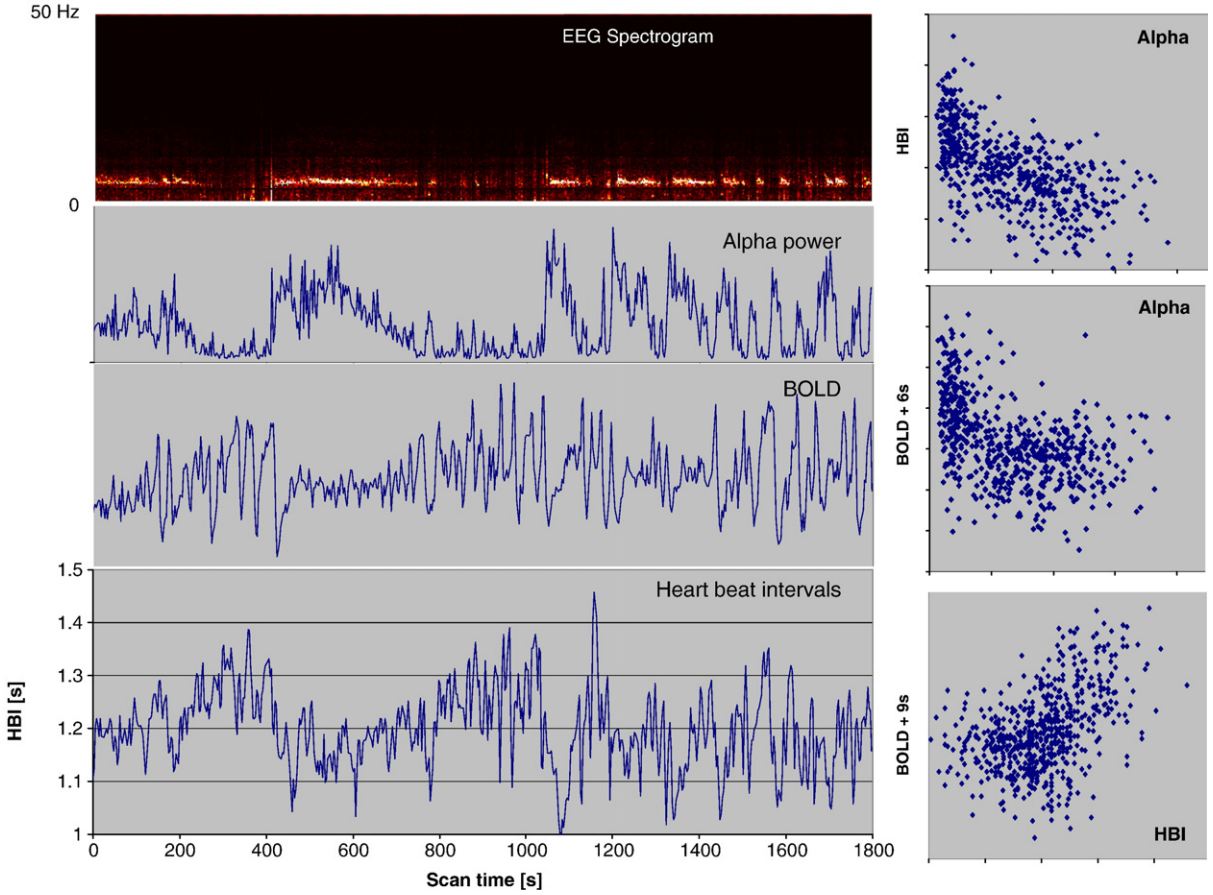

Fig. 2. Top row shows the spectrogram of subject 9, and immediately below the alpha band variations (averaged from 9.0 to 11.0 Hz) are shown in arbitrary units (AU). Next row shows a sample of a BOLD signal (AU) from an occipital point where both high correlations with alpha power and HBI were found. Bottom row shows heart beat intervals [s]. This subject shows a very strong negative correlation between alpha power and HBI ($r = -0.61$). On the right the scatter plots of alpha versus HBI, alpha versus BOLD and HBI versus BOLD are shown. In these scatter plots the BOLD signal was shifted over a multiple of TR to obtain maximum amount of correlation.

subject's alpha peak frequency, and averaging the seven frequency components within this 2 Hz. band. Six motion regressors were derived from the three rotation and three translation parameters of the fMRI motion correction (Friston et al., 1996). Data points coinciding with artificially large alpha power or an amount of motion larger than 0.05 cm or 0.5° were excluded from the analysis. Dependent on the assumed length of the hemodynamic response also neighbouring data points were excluded. Glover's (2000) RETROICOR method with three sines and three cosines was used to obtain six regressors related to the phase of the heart beat at the moment a slice was acquired. Furthermore, an offset, a linear and a quadratic trend were added to the regressors. Therefore, apart from the alpha band regressors and heart beat interval regressors described below, a total of 15 regressors were used as confounders.

In addition to the *phase* of the heart beat, which is the basis of RETROICOR, we also considered the *rate* of the heart beat. However, to simplify construction of regressors, we consider heart beat intervals (HBI), defined as the time between two heart beats derived from ECG or pulse. Since these interval times are irregularly sampled over time they cannot be directly used as regressor. Therefore, at the onset of each slice acquisition, an interval of T_{av} was defined, over which the heart beat intervals were averaged. The regressor so obtained was shifted in time over multiples of TR, to account for possible delayed responses of the fMRI signal on heart beat variations. Because we anticipate fast responses, a regressor was defined for each separate slice (and not merely for each volume), by taking into account the fact that slices were acquired at slice varying onset times linearly varying from bottom to top. Therefore, contrary to Shmueli et al. (2007), the estimated regression coefficients are intrinsically corrected for different slice times. To reduce confusion we stress that these HBI regressors represent the inverse of heart rate.

For both Glover's regressors and the HBI regressors time markers are needed that indicate heart beats. Because one cannot rely completely on automatic detection algorithms to find these markers automatically, visual inspection is required to edit erroneous peak detections. In such cases the editing was based on the inspection of both ECG, pulse and cardio ballistic artefacts in the EEG.

Correlation analysis

Similar to the analysis presented in De Munck et al. (2007a) regressors were correlated to fMRI by shifting them over time and introducing an unknown regression coefficient for each time shift, as shown in Eq. (1).

$$\mathrm{BOLD}_j = \sum_{n=N_{\mathrm{Start}}}^{N_{\mathrm{End}}-1} r_n \mathrm{HBI}_{j-n} + \sum_{m=M_{\mathrm{Start}}}^{M_{\mathrm{End}}-1} a_m \mathrm{ALPHA}_{j-m} + \sum_{m=M_{\mathrm{End}}}^{M_{\mathrm{End}}+14} \beta_m \mathrm{CONF}_{m,j} + \varepsilon_j \quad (1)$$

In this equation r_n represents the fMRI impulse response to HBI variations, and α_m represents the alpha band impulse response function. Because slice time corrected regressors were used, no slice time correction on the estimated response curves is required. When studying the correlation between fMRI and HBI, the shifted alpha band power was used as a confounder, in addition to the other 15 regressors of non-interest defined above. In this case, there were $N_{\mathrm{End}} - N_{\mathrm{Start}}$ regressors of interest, whose significance was tested with an F-test, thereby accounting for $M_{\mathrm{End}} - M_{\mathrm{Start}} + 15$ regressors of non-interest (confounders). Conversely, when studying the alpha band response, the roles of the HBI and alpha band regressors were interchanged, and there were $M_{\mathrm{End}} - M_{\mathrm{Start}}$ regressors of interest, and $N_{\mathrm{End}} - N_{\mathrm{Start}} + 15$ confounders. This procedure assured that in both studies, the estimated parameters were identical, and that different sets of parameters of the same model were compared. In our previous study (De Munck et al., 2007a), alpha response functions were studied while ignoring the HBI regressors. Therefore, results in that study might be biased by an unmodelled heart rate effect, that could explain part of the observed correlation, and that also could disturb the estimated alpha response function. In all the analysis presented here, $N_{\mathrm{Start}} = M_{\mathrm{Start}} = -2$ and $N_{\mathrm{End}} = M_{\mathrm{End}} = 8$ was taken (so 10 shifts were included).

The correlation between observed data and regressors of interest (either shifted HBI-functions or shifted alpha band profiles) was determined by computing the correlation coefficient between data and predicted signal, after projecting out the confounders from both the data and the regressors of interest. Under the NULL hypothesis that all parameters of interest are zero (hence that the data is fully explained by nuisance effects), the statistical significance of the correlation coefficient is determined using an F-test, accounting for the number of estimated parameters, the number nuisance effects and the number of data points. Mathematical details can be found e.g. in appendix A of De Munck et al. (2007a). Therefore, contrary to Shmueli et al. (2007) who used different t-tests for different slice delays, the impulse response function is determined with a single regression model, with a single statistical test.

Regression analysis was performed voxel wise, for all voxels corresponding to the brain, as determined by a simple thresholding

Table 1
The first column is the subject number

Subject	Correlation alpha HBI	HBI [s]	Fraction activated brain		
			HBI as regressor alpha as confounder	Alpha as regressor, HBI as confounder	Alpha as regressor alone
1	$-0.33^{(**)}$	0.86	0.26	0.27	0.29
2	$-0.24^{(**)}$	1.40	0.08	0.42	0.42
3	$-0.18^{(**)}$	0.90	0.75	0.01	0.03
4	$-0.43^{(**)}$	1.21	0.61	0.26	0.34
5	$-0.40^{(**)}$	1.19	0.58	0.68	0.77
6	+0.01	0.78	0.61	0.04	0.06
7	$-0.30^{(**)}$	1.21	0.35	0.44	0.48
8	$-0.19^{(**)}$	0.81	0.32	0.28	0.14
9	$-0.61^{(**)}$	1.20	0.82	0.82	0.89
10	+0.03	1.18	0.23	0.08	0.04
11	$-0.22^{(**)}$	1.01	0.94	0.69	0.59
12	$-0.53^{(**)}$	1.04	0.77	0.26	0.74
13	$-0.33^{(**)}$	0.82	0.78	0.61	0.75
14	$-0.20^{(**)}$	1.02	0.47	0.16	0.25
15	−0.01	0.86	0.54	0.03	0.01
16	$-0.13^{(**)}$	0.98	0.47	0.01	0.01

Second column gives the Pearson correlation coefficient between alpha band and HBI regressor. Here (**) indicates $p \ll 1\%$. Third column gives the average HBI in s. The last three columns present the fraction of active brain volume, defined as those points that are declared active at an FDR threshold of 1% in different conditions. In the first of these columns, shifted HBI regressors were used and shifted alpha power as confounders. In the second, the roles of HBI regressors and alpha power were reversed, and in the last column, shifted alpha power was used without adding heart rate confounders.

operation on the smoothed fMRI scans. The resulting array of p-values was converted to a false detection rate (FDR) using the Benjamini and Hochberg (1995) procedure (see also Genovese et al., 2002). Then FDR-images were thresholded and the correlations of the subthreshold points were overlaid onto the anatomical MRI scan. To quantify the fraction of the brain volume that significantly correlated to the regressors of interest, the number of points below an FDR threshold of 1% were divided by the total number of brain points.

Heart beat response shapes

To study regional differences between estimates $\hat{r}_j$ of r_j a hierarchical clustering analysis was applied, similar to that used by De Munck et al. (2007a). Briefly, a distance table was computed consisting of the distances between estimated and normalised response curves at different voxels. Clustering analysis was done exclusively on voxels surviving the 10% FDR threshold. For subjects where this threshold yielded more than 8000 significant points, only the 8000 most significant points were included in cluster analysis, to avoid computer memory overflow in the computation of the distance table. This way of selecting points of interest resulted in a comparable number of points for different subjects, but avoids inclusion of non-significant ones. Cluster analysis yielded groups of pixels in which the response curves are as similar as possible. The cluster centres, i.e. the cluster averaged responses, were used as representative for that region. Cluster analysis was performed for each subject individually. Retrospectively, clusters were colour coded in such a way that clusters found in different subjects receive the same colours when they correspond to more or less the same response function.

Note that for cluster analysis a higher FDR threshold (maximum 10%) was used in some subjects than in the quantification of the amount of correlation (1%). We think this approach is justified because only cluster averages are compared over subjects. The large cluster sizes we used reduce the extra noise due to the higher threshold.

Results

Fig. 2 (left) presents from top to bottom the spectrogram of subject 9, the alpha band regressor derived from thereof, a sample of a BOLD signal from an occipital point and the HBI regressor. These HBI variations are computed over the 2s interval starting at the onset of the first slice. In this case the correlation between HBI variations and the alpha band is very high (− 0.61), as can be observed from the scatter plot presented in the upper right panel of Fig. 2. Note that the negative correlation implies that epochs with higher alpha power coincide with a higher heart rate and vice versa. The other two scatter plots of Fig. 2 present the combinations of alpha power and BOLD, and HBI and BOLD, respectively. Correlations between alpha band power and HBI variations for other subjects are presented in Table 1, second column. It appears that in most subjects a highly significant negative correlation between alpha power and heart beat intervals exist.

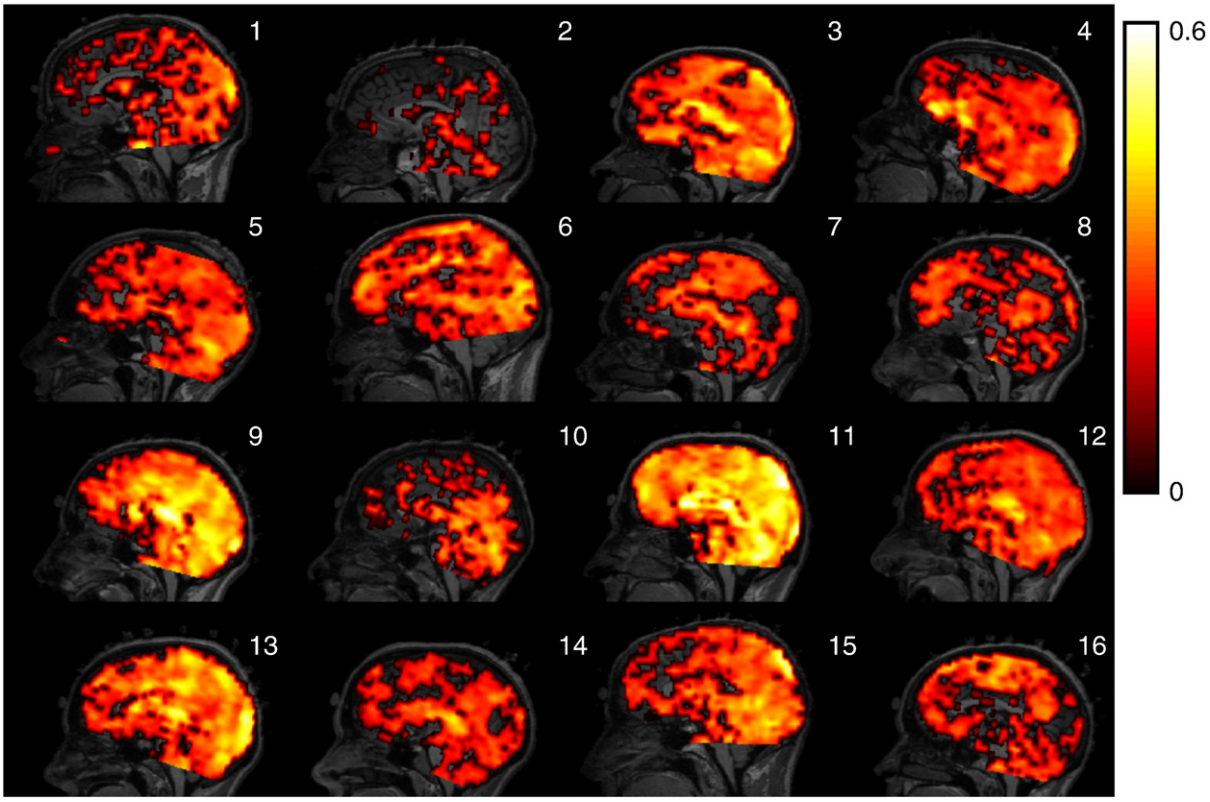

Fig. 3. The correlation between fMRI signal and HBI variations. Of each subject the mid sagittal slice of the anatomical scan is presented, overlaid with a thresholded and colour coded correlation coefficient. In the correlation analysis, the (shifted) alpha power was taken as confounders. The correlation threshold corresponds to an FDR of 1%, and this threshold is computed for each subject individually. On the right the meaning of the colour scale is given. (For interpretation of the references to colour in this figure legend, the reader is referred to the web version of this article.)

Heart beat intervals also correlate substantially to the fMRI signals, as follows from Fig. 3. This figure presents the mid sagittal planes of the anatomical MR scan of each subject overlaid with a thresholded partial correlation coefficient. The threshold used corresponds to a false detection rate of 1%, adapted to the data of each individual subject. It appears that HBI variations are correlated to fMRI over very large parts of the brain. However, there is some variation over subjects, as quantified in Table 1.

The last three columns of Table 1 present the fractions of activated brain volume at an FDR of 1%, that emerge for different regressors of interest and confounders. Column 4 contains the fraction of active brain, corresponding to the maps in Fig. 3 and Eq. (1): shifted heart beat intervals as regressors of interest, and shifted alpha band regressors as confounders in addition to the other confounders. In column 5 the roles of the alpha band and heart beat intervals are reversed. There appears to be a large inter-subject variation in the part of the brain that is involved in the generation of the alpha band. When the heart beat interval confounders are omitted, as was done in previous EEG/fMRI studies, the estimated fraction of points in the alpha band generally changed only slightly (column 6), with the notable exception of subject 12, where the estimated active fraction is three times as large when heart beat interval confounders are omitted. Note that this subject also shows a very strong correlation of heart beat interval regressors and alpha power (− 0.53).

Cluster analysis of the response shapes was truncated at 2 clusters as shown in Fig. 4, because from visual inspection it appeared that further subdividing the response shapes did not yield much more variation. The time scale starts at 6 s before the HBI averaging window and extends to 21 s. after that. The cluster averaged response shapes appear to be quite consistent over subjects. Cluster 1 (green) peaks negatively after 3 s and cluster 2 (red) also peaks negatively but after 6 s. Also, the response of cluster 2 is larger than that of cluster 1. The grant averaged impulse responses (left part) seem to show a systematic increase at 0s, and hardly any response for negative times. However, these observations were not tested formally.

Fig. 5 presents the spatial distribution of the clusters for an arbitrary subset of 4 subjects (4, 8, 12 and 16). The overlaid colours (green and red) correspond to the different response shapes. It appears that late response (cluster 2, red) includes the ventricles and cluster 1 is more representative for points within brain tissue. Note however, that due to the memory limitations of our computers, clustering analysis was restricted to the 8000 most significant points, (25% of the brain volume) and from Table 1 it appears that in many subjects much larger parts of the brain correlate to heart beat variations.

Clustering analysis truncated at more than 2 clusters resulted in splitting of cluster 1, but in a way that is not consistent over subjects. To study the reproducibility of the HBI correlation patterns and the HBI-response curves, within a single subject, a control experiment was performed with subject 5, using exactly the same experimental setup and data analysis, with the exception that recording time was 20 min instead of 30 min. The control experiment was performed after all data of the other subjects were acquired. Clustering results are shown in Fig. 6, where the top panels depict the control experiment (20 min), and the bottom panels the regular one (30 min). Cluster analysis of the most significant areas was now truncated at 4

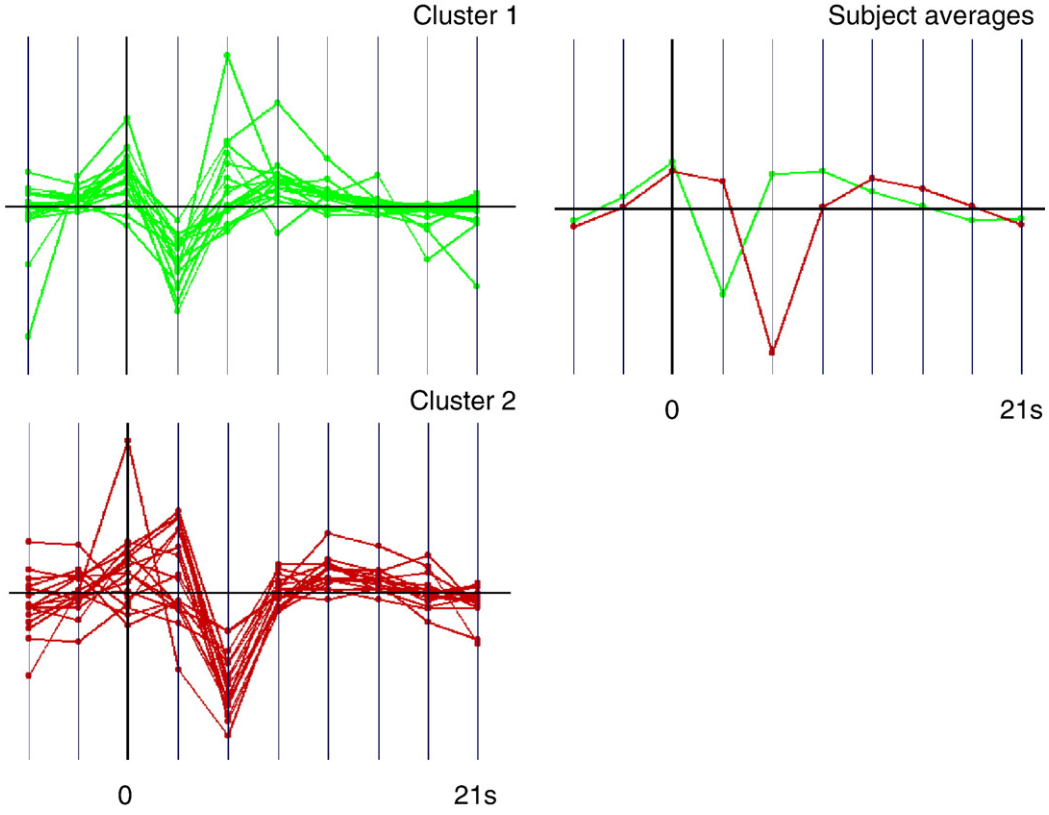

Fig. 4. Cluster averaged HBI-response curves are shown in arbitrary units. Clustering was stopped at 2 clusters per subject and at the left the responses curves for all different subjects are overlaid. The right hand side shows the grand averages.

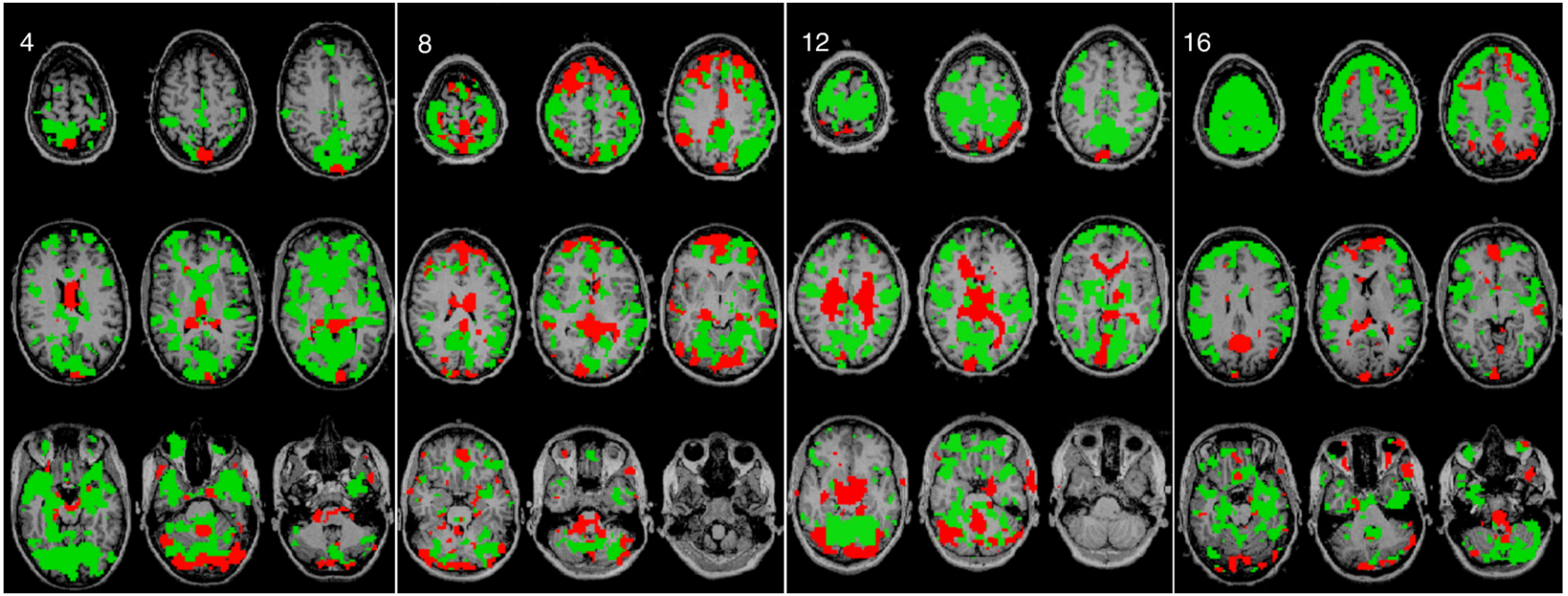

Fig. 5. The spatial distributions of the response curves are presented for four arbitrarily chosen subjects (4, 8, 12 and 16) and overlaid onto the anatomic scan. It appears that cluster 2 includes the ventricles and other parts of the cerebrospinal fluid and cluster 1 is more representative for the brain. Note that because of memory restrictions in the cluster analysis, cluster analysis is applied only on the most significant part of the responses curves, and a much larger part of the brain can be correlated to HBI-intervals than this figure suggests (see Table 1).

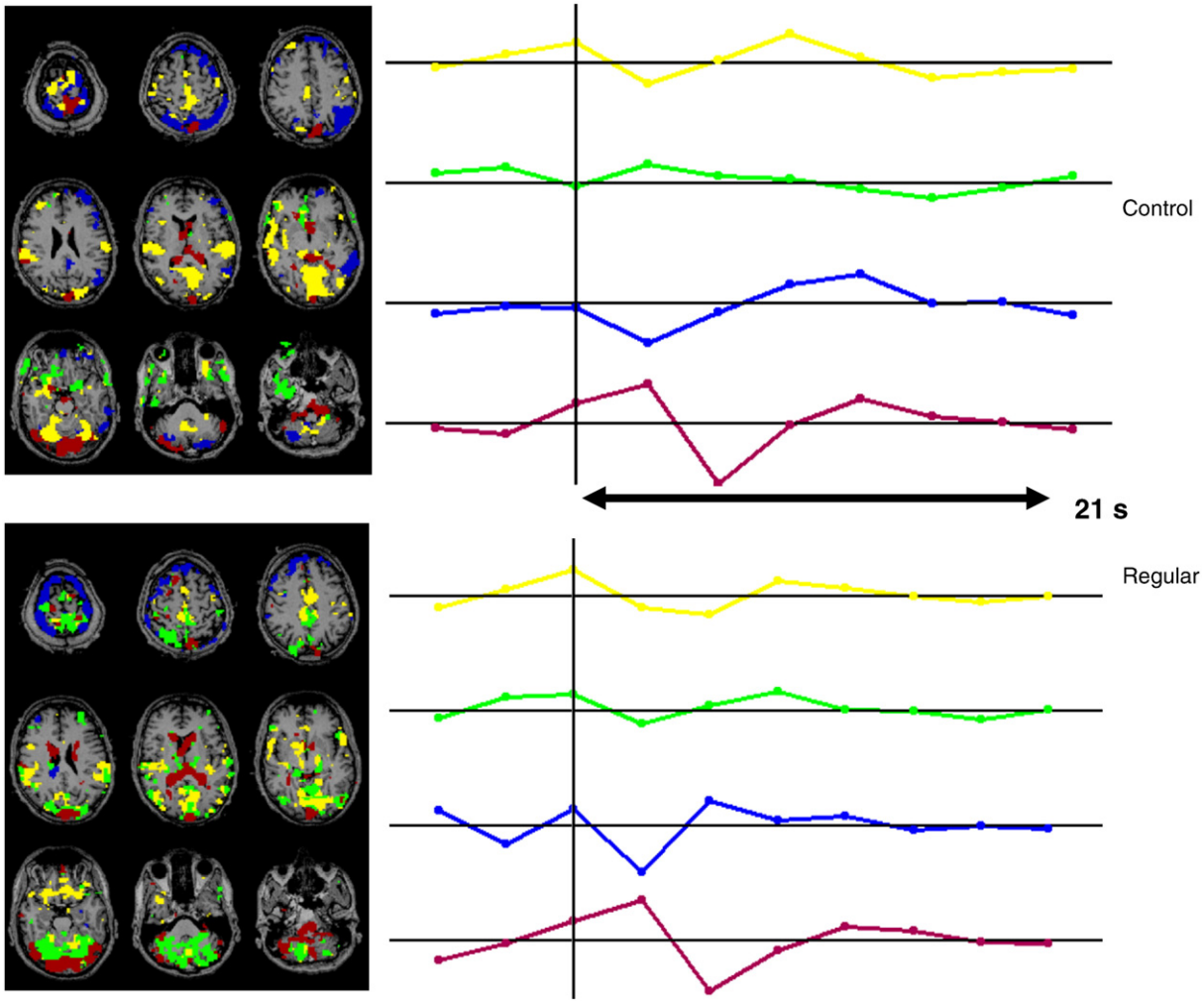

Fig. 6. Results of a regular experiment of subject 5 (bottom) compared to those of a control experiment(top) in the same subject. On the left the significantly correlated areas are presented, colour coded according to the local response curves to heart beat variations. It appears that both data sets, and also the clusters show similarity. On the right the response curves [AU] are plotted in colours corresponding to the spatial clusters.

clusters, which in both data sets resulted in two brain clusters (green and yellow), a cluster including the ventricle (red) and a cluster including brain and superficial CSF (blue). It appears that, apart from the separation into brain clusters, the spatial distribution of the remaining clusters and their response curves, are quite well reproducible.

Discussion

Our experiments and data analysis demonstrate that large part of the fMRI brain signals correlate to variations in heart beat intervals. These correlations appear to be quite reproducible within one subject and over different subjects. Shmueli et al. (2007), who used a 3T scanner and a TR of 6 s, have found substantial variations over subjects. An important finding is that, despite the fact that Glover's (2000) RETROICOR regressors were included, a substantial correlation between HBI and fMRI signals at the cerebrospinal fluid remains. We explain this finding by the complementary nature of Glover's model and our HBI-model. In Glover's model the heart beat artefact is described as a non-linear function of the *instantaneous phase* of the heart beat, whereas our HBI-regression model is based on the *heart rate* and time delays thereof. Apparently, the instantaneous phase model is too restricted for a complete description of the heart beat effect on the CSF. Inspection of the response curves shows that at least some time delays are required to describe fMRI signals in terms of HBI variations. We expect this finding will be useful to disentangle the precise mechanism by which heart beat and respiration affect the fMRI signals (Windischberger et al., 2002).

Similarly to Shmueli et al. (2007), our study shows that HBI variations do not only correlate well within "artefact" regions like CSF, ventricles and large vessels, but also within brain tissue itself. In principle, this finding can have serious impact on the way BOLD responses are to be interpreted when paradigms are used where heart rate variations are modulated by the experimental stimulus. In a different context, such modulation has been demonstrated when stimuli with an emotional load are used (e.g. Foster and Harrison, 2004; Critchley et al., 2005). This may happen in experimental paradigms where the resting state is compared to a task requiring cognitive processes with emotional features. In such cases, standard fMRI correlation analyses yield activation and deactivation maps that are interpreted as local changes in oxygen consumption due to specific local brain activity associated with the cognitive tasks. Our data suggests that an alternative explanation could be provided by a

general, non-specific, hemodynamic response to variations in heart beat intervals, evoked by the task. In the same line of thought one could hypothesize that the deactivation of the "default network", being a structure that deactivates during a very generic class of experimental paradigms (Shulman et al., 1997), is a heart rate related hemodynamic effect in the brain. However, considering that the correlation maps depicted in Fig. 3 are very different from the default network, and that the response curves depicted in Fig. 4 are also different from the canonical HRF used in fMRI analysis, we conclude that heart rate effects can only provide a part of the explanation for the behaviour of the default network. To find further support for this conclusion, the heart rate regressor was convolved with the canonical hemodynamic response function instead of a response function estimated from the data. The fraction of activated brain volume became much smaller than in Table 1, column 4, and no evidence for an exclusive involvement of the default network was found.

In the present study no external stimuli were examined that modulate heart beat intervals. Therefore, the impact of this modulation on fMRI correlation analysis was not tested directly. Instead fMRI-alpha band correlations were re-explored, using shifted HBI as confounders. Because we also found that correlations between alpha power and HBI are generally quite substantial, one could expect that, for instance, the estimated fraction of the activated brain would be reduced when these confounders are used, compared to our previous analysis where they were ignored. From the last two columns of Table 1 it appears that this effect is not very large, except for one subject (# 12). On the other hand, we would also like to stress that the inclusion of HBI regressors in the data analysis is relatively a small computational effort, and therefore we recommend their inclusion once the ECG or pulse is co-registered in fMRI experiments.

The use of an incomplete model where the coupling between HBI and the regressors of interest is ignored, may not only influence the estimated fraction of active voxels, but it may also affect the estimated shape of the HRF. For instance, in De Munck et al. (2007a) it was found that, contrary to the cortex, the estimated alpha response function of the thalamus has a bi-phasic character. Because, in that work the HBI-alpha power regressors were left out, these deviant responses might be considered as an artefact, caused by the use of an incomplete response model. However, a comparison of the subject-averaged alpha response functions shows (Fig. 7) that the bi-phasic character of the thalamic alpha response functions remains when HBI regressors are included as confounders. Therefore, if these response shapes are a heart beat artefact, then the underlying model must be more complicated than shifted heart beat intervals combined with a non-linear transformation of the heart beat's phase.

The primary goal of our experiments was to study the brain's state when subject is at rest, but not asleep. The observed heart rate variations confirm that the resting state is far from being a passive state. To a large extent heart rate variations are correlated to the respiration cycle, causing variations in vascular resistance which are compensated by variations in blood pressure and therefore heart rate. An additional effect of heart rate variations is to adjust the supply of oxygen to the needs evoked by subject's mental and physical efforts. We interpret our observed HBI-alpha power correlations as a manifestation of this cardiac brain coupling. However, since alpha power is reduced when a subject is mentally active, and it is enhanced in the absence of such activity (e.g. Lindsley, 1952; Stennett, 1957; Klimesch, 1999), it seems counter intuitive at first glance that alpha power is *negatively* correlated to heart beat intervals. We explain this "paradox" by the assumption that in most subjects, brain states during quite wakefulness vary between wakefulness and drowsiness. This hypothesis is supported by the fact that many subjects after the experiment spontaneously reported difficulty with staying awake. Since the alpha rhythm also disappears during sleep whereas heart rate slows down, this variation between mental states would explain the observed sign of correlation found in most subjects. In this sense the alpha rhythm represents a "standby" mode of the brain, rather than a resting state. This interpretation is consistent with the inverted U-relationship between alpha amplitude and a "behavioural continuum" of states of the organism (Lindsley, 1952; Stennett, 1957). The implication of this interpretation is, that even in our paradigm, which is a very standard resting state paradigm, such "behavioural continuum" of states exists.

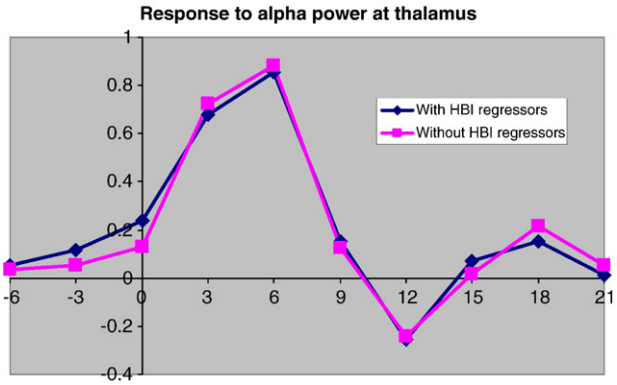

Fig. 7. The effect of including HBI confounders in estimating the alpha response curves (AU) at the thalamic region is shown. In both situations, including and excluding HBI regressors, the alpha response curves were averaged over those subjects, where the response was found significant at and FDR level of 1%.

References

Benjamini, Y., Hochberg, Y., 1995. Controlling the false discovery rate: a practical and powerful approach to multiple testing. J. R. Stat. Soc., B 57 (1), 289–300.

Buckner, R.L., Vincent, J.L., 2007. Unrest and rest: default activity and spontaneous network correlations. NeuroImage 37, 1091–1096.

Buxton, R.B., Uludağ, K., Dubowitz, D.J., Liu, T.T., 2004. Modeling the hemodynamic response to brain activation. NeuroImage 23, S220–S233.

Critchley, H.D., Rotshtein, P., Nagai, Y., O'Doherty, J., Mathias, C.J., Dolan, R.J., 2005. Activity in the human brain predicting differential heart rate responses to emotional facial expressions. NeuroImage 24, 751–762.

Damoiseaux, J.S., Rombouts, S.A.R.B., Barkhof, F., Scheltens, P., Stam CJ Smith, S.M., Beackmann, C.F., 2006. Consistent resting-state networks across healthy subjects. PNAS 103 (37), 13848–13853.

De Munck, J.C., Gonçalves, S.I., Huijboom, L., Kuijer, J.P.A., Pouwels, P.W.J., Heethaar, R.M., Lopes da Silva, F.H., 2007a. The hemodynamic response of the alpha rhythm: an EEG/fMRI study. NeuroImage 35 (3), 1142–1151.

De Munck, J.C., Gonçalves, S.I., Faes Th, J.C., Pouwels, P.J.W., Kuijer, J.P.A., Heethaar, R.M., Lopes da Silva, F.H., 2007b. The relation between alpha band power, heart rate and fMRI. Proceedings of fourth IEEE International Symposium on Biomedical Imaging, 2007, Arlington, Virginia.

Ehrhart, J., Toussaint, M., Simon, C., Gronfier, C., Luthringer, R., Brandenberger, G., 2000. Alpha activity and cardiac correlates: three

types of relationships during nocturnal sleep. Clin. Neurophysiol. 111, 940–946.
Foster, P.S., Harrison, D.W., 2004. The covariation of cortical electrical activity and cardiovascular responding. Int. J. Psychophysiol. 52 (3), 239–255.
Fox, P.T., Raichle, M.E., 1986. Focal physiological uncoupling of cerebral blood flow and oxidative metabolism during somatosensory stimulation in human subjects. Proc. Natl. Acad. Sci. U.S.A. 83, 1140–1144.
Frigo, M., Johnson, S.G., 2005. The design and implementation of FFTW. Proceedings of the IEEE, vol. 93(2), pp. 216–231.
Friston, K.J., Williams, S., Howard, R., Frackowiak, R.S., Turner, R., 1996. Movement-related effects in fMRI time-series. Magn. Reson. Med. 35, 346–355.
Genovese, C.R., Lazar, N.A., Nichols, T., 2002. Thresholding of statistical maps in functional neuroimaging using the false discovery rate. NeuroImage 15, 870–878.
Glover, G.H., Li, T.Q., Ress, D., 2000. Image-based method for retro-sspective correction of physiological motion effects in fMRI: RETRO-ICOR, MRM 44, 162-167.
Goldman, R.I., Stern, J.M., Engel Jr., J., Cohen, M., 2002. Simultaneous EEG and fMRI of the alpha rhythm. NeuroReport 13 (18), 2487–2492.
Gonçalves, S.I., de Munck, J.C., Pouwels, P.J.W., Schoonhoven, R., Kuijer, J.P.A., Maurits, N.M., Hoogduin, J.M., Van Someren, E.J.W., Heethaar, R.M., Lopes da Silva, F.H., 2006. Correlating the alpha rhythm to BOLD using simultaneous EEG/fMRI: inter-subject variability. NeuroImage 30 (1), 203–213.
Gonçalves, S.I., Pouwels, P.J.W., Kuijer, J.P.A., Heethaar, R.M., de Munck, J.C., 2007. Artifact removal in co-registered EEG/fMRI by selective average subtraction. Clin. Neurophysiol. 118, 2437–2450.
Greicius, M.D., Krasnow, B., Reiss, A.L., Menon, V., 2003. Functional connectivity in the resting brain: a network analysis of the default mode hypothesis. PNAS 100 (1), 253–258.
Gusnard, D.A., Raichle, M.E., 2001. Searching for a baseline: functional Imaging and the resting human brain. Nat. Rev., Neurosci. 2 (10), 685–694.
Herscovitch, P., Markham, J., Raichle, M.E., 1973. Brain blood flow measured with intravenous $H_2^{15}O$ I. Theory and error analysis. J. Nucl. Med. 24 (9), 782–789.
Klimesch, W., 1999. EEG alpha and theta oscillations reflect cognitive and memory performance: a review and analysis. Brain Res. Rev. 29, 169–195.
Kubota, Y., Sato, W., Toichi, M., Murai, T., Okada, T., Hayashi, A., Sengoku, A., 2001. Frontal midline theta rhythm is correlated with cardiac autonomic activities during the performance of an attention demanding meditation procedure. Cogn. Brain Res. 11 (2), 281–287.
Kwong, K.K., 1995. Functional magnetic resonance imaging with echo planar imaging. Magn. Reson. Q. 11 (1), 1–20.
Laufs, H., Krakow, K., Sterzer, P., Eger, E., Beyerle, A., Salek-Haddadi, A., Kleinschmidt, A., 2003a. Electroencephalographic signatures of attentional and cognitive default modes in spontaneous brain fluctuations at rest. PNAS 100 (19), 11053–11058.
Laufs, H., Kleinschmidt, A., Beyerle, A., Eger, E., Salek-Haddadi, A., Preibisch, C., Krakow, K., 2003b. EEG-correlated fMRI of human alpha activity. NeuroImage 19, 1463–1476.
Laufs, H., Lengler, U., Hamandi, K., Kleinschmidt, A., Krakow, K., 2006. Linking generalized spike-and-wave discharges and resting state brain activity by using EEG/fMRI in a patient with absence seizures. Epilepsia 47 (2), 444–448.
Liston, A.D., De Munck, J.C., Hamandi, K., Laufs, H., Ossenblok, P., Lemieux, L., 2003a. Analysis of EEG-fMRI of epileptiform discharges based on automated classification of interictal epileptiform discharges. NeuroImage 31 (3), 1015–1024.
Liston, A.D., Lund, T.E., Salek-Haddadi, A., Hamandi, K., Friston, K.J., Lemieux, L., 2003b. Modelling cardiac signal as a confound in EEG-fMRI and its application in focal epilepsy studies. NeuroImage 30, 827–834.
Lindsley, D.B., 1952. Psychological phenomena and the electroencephalogram. Electroencephalogr. Clin. Neurophysiol. 4 (4), 443–456.
Logothetis, N.K., 2007. The ins and outs of fMRI signals. Nat. Neurosci. 10 (10), 1230–1231.
Logothetis, N.K., Pauls, J., Augath, M., Trinath, T., Oeltermann, A., 2001. Neurophysiological investigation of the basis of the fMRI signal. Nature 412, 150–157.
Lund, T.E., Madsen, K.H., Sidaros, K., Luo, W.L., Nichols, T.E., 2006. Non-white noise in fMRI: does modelling have an impact? NeuroImage 29, 54–66.
Lemieux, L., Allen, P.J., Franconi, F., Symms, M.R., Fish, D.R., 1997. Recording of EEG during fMRI experiments: patient safety. MRM 38, 943–952.
Lemieux, L., Allen, P.J., Krakow, K., Symms, M.R., Fish, D.R., 1999. Methodological issues in EEG-correlated functional MRI experiments. IJBEM 1 (1), 87–95.
Mantini, D., Perrucci, M.G., Del Gratta, C., Romani, G.L., Corbetta, M., 2007. Electrophysiological signatures of resting state networks in the human brain. PNAS 104 (32), 13170–13175.
Mazoyer, B., Zago, L., Mellet, E., Bricogne, S., Etard, O., Houdé, O., Crivello, F., Joliot, M., Petit, L., Tzourio-Mazoyer, N., 2001. Cortical networks for working memory and executive functions sustain the conscious resting state in man. Brain Res. Bull. 54 (3), 287–298.
Moosmann, M., Ritter, P., Krastel, I., Brink, A., Thees, S., Blankenburg, F., Taskin, B., Obrig, H., Villringer, A., 2003. Correlates of alpha rhythm in functional magnetic resonance imaging and near infrared spectroscopy. NeuroImage 20, 145–158.
Morcom, A.M., Fletcher, P.C., 2007. Does the brain have a baseline? Why we should be resisting a rest. NeuroImage 37, 1073–1082.
Ogawa, S., Tank, D.W., Menon, R., Ellermann, J.M., Kim, S.G., Merkle, H., Ugurbil, K., 1992. Intrinsic signal changes accompanying sensory stimulation: functional brain mapping with magnetic resonance imaging. PNAS 89 (13), 5951–5955.
Raichle, M.E., Snyder, A.Z., 2007. A default mode of brain function: a brief history of an evolving idea. NeuroImage 37, 1083–1090.
Raichle, M.E., MacLeod, A.M., Snyder, A.Z., Powers, W.J., Gusnard, D.A., Shulman, G.L., 2001. A default mode of brain function. PNAS 98 (2), 676–682.
Salek-Haddadi, A., Friston, K.J., Lemieux, L., Fish, D.R., 2003. Studying spontaneous EEG activity with fMRI. Brain Res. Rev. 43, 110–113.
Shulman, G.L., Fiez, J.A., Corbetta, M., Buckner, R.L., Miezin, F.M., Raichle, M.E., Petersen, M.E., 1997. Common blood flow changes across visual tasks: II. Decreases in cerebral cortex. J. Cogn. Neurosci. 9 (5), 648–663.
Shmueli, K., Van Gelderen, P., De Zwart, J., Horovitz, S.G., Fukanaga, M., Jansma, J.M., Van Duyn, J.F., 2007. Low frequency fluctuations in the cardiac rate as a source of variance in the resting state fMRI BOLD signal. NeuroImage 38, 306–320.
Stennett, R.G., 1957. The relationship of alpha amplitude to the level of palmar conductance. Electroencephalogr. Clin. Neurophysiol. 9 (1), 131–138.
Vincent, J.L., Patel, G.H., Fox, M.D., Snyder, A.Z., Baker, J.T., Van Essen, D.C., Zempel, J.M., Snyder, L.H., Corbetta, M., Raichle, M.E., 2007. Intrinsic functional architecture in anaesthetized monkey brain. Narure 447 (3), 83–86.
Windischberger, C., Langenberger, H., Sycha, T., Tschernko, E.M., Fuchsjger-Mayerl, G., Schmetterer, L., Moser, E., 2002. On the origin of respiratory artifacts in BOLD-EPI of the human brain. Magn. Reson. Imaging 20, 575–582.
Zijlmans, M., Huiskamp, G., Hersevoort, M., Seppenwoolde, J.H., Van Huffelen, A.C., Leijten, F.S.S., 2007. EEG-fMRI in the preoperative work-up for epilepsy surgery, Brain. Brain 130, 2343–2353.